



Simplified macro-modelling for predicting seismic response of bridges with dissipative controlled rocking connections

M. Mashal

Idaho State University, Idaho, United States

A. Palermo

University of Canterbury, Christchurch

ABSTRACT

In a typical dissipative controlled rocking (DCR) connection, unbonded post-tensioning is combined with internal or external dissipaters to provide self-centring and energy dissipation, respectively. DCR connections are gaining popularity in buildings and bridges within the context of low damage seismic design. Over the years, there have been many procedures proposed for modelling the response of DCR connections. These include the lumped plasticity, multi-spring, fibre element, and finite element models. The lumped plasticity model offers a simplified analytical tool to capture the seismic response of a DCR connection under lateral loads. This model uses rotational springs to model the moment-rotation response of the elements in a DCR connection. In this type of modelling, two rotational springs, one representing the unbonded post-tensioning, and the other the energy dissipaters, are used in parallel. The springs have zero lengths, and all inelastic behaviour assumed to be concentrated at the connection region where the rotational springs are located. The overall flag-shaped hysteretic response of the DCR connection can be obtained by summing the contributions from the two springs. In this research, lumped plasticity models are used to capture the seismic response of a precast bent with DCR connections. The half-scale bent was tested under a series of quasi-static cyclic loading with or without axial loads and external dissipaters. Two types of external dissipaters, grooved dissipaters and mini UFP dissipaters, were tested in the bent. Analytical results for the bent using lumped plasticity models are shown to be in good agreements with experimental results.

1 INTRODUCTION

Over the last 15 years, there have been many procedures proposed for modelling the response of dissipative controlled rocking (DCR) connections. These are briefly discussed here.

1.1 Lumped Plasticity Model

Lumped plasticity model uses rotational springs to construct the moment-rotation response of the elements in a post-tensioned rocking system. Past references on this type of modelling for DCR connections include (Kurama et al. 1999), (Pampanin et al. 2001), (fib 2003), and (Palermo et al. 2005¹). In a lumped plasticity model, two rotational springs are placed in parallel with zero length. The springs are intended to represent the response of the unbonded post-tensioning and dissipaters at the rocking interface. The inelastic behaviour is assumed to be concentrated at the connection region only. Precast elements are modelled as elastic members. Section analysis of the rocking interface would be required to construct the monotonic response of the unbonded post-tensioning and dissipaters. The effect of gravity (axial load) can be combined with the post-tensioning spring. Bilinear or trilinear backbone curves can be used to construct the response of the springs that represent post-tensioning and dissipaters. The summation of the responses from the springs will be the overall response of the system.

Lumped plasticity models are simplified tools to obtain the response of DCR connections. They generally do not require any special or sophisticated software. Using the procedure outlined in the PRESSS Design Handbook (Pampanin et al. 2010), simple spreadsheets can be used to obtain the backbone curves required to generate the pushover envelope and hysteretic response of bridges with DCR connections. Figure 1 presents a sample lumped plasticity model for a cantilever pier with DCR connection at the base.

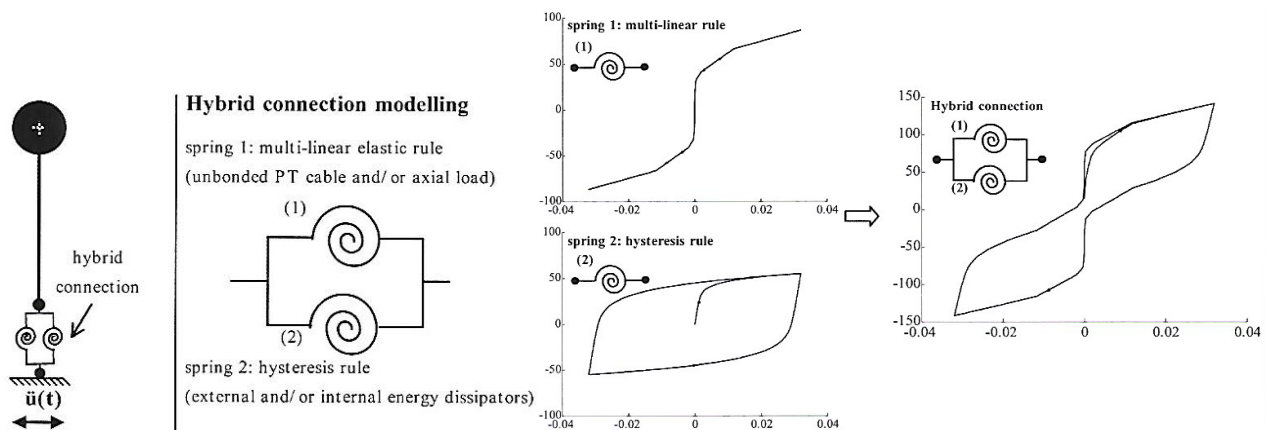


Figure 1: Lumped plasticity model for DCR connection (Palermo et al. 2005)

1.2 Multi-Spring Model

This model is more complicated. It initially used two axial springs that were located at the rocking interface. It was developed to capture the response of rocking walls (Conley et al. 1999). The axial springs are elastic compression-only (gap elements) which are intended to capture the actual rocking response of the wall as the wall uplifts on one end. The response of post-tensioning and dissipaters are modelled using additional springs with hysteretic response. This model was concluded to overestimate the tendon elongation and internal moment non-conservatively. Therefore, it was subsequently refined by Marriott (2009). Follow up research on multi-spring models by (Kim 2002), (Spieth et al. 2004), and (Palermo et al. 2005²), incorporated multiple axial springs that were distributed along the rocking interface. The multi-spring element has been added in the inelastic program called "Ruaumoko" (Carr, 2004) as shown in Figure 2a. Figure 2b presents analytical model of a rocking pier using multi-spring element from (Marriott 2009). In general multi-spring

models provide better results, especially when vertical excitation is present in the rocking system. However, they can be time consuming due to calibration of each spring properties.

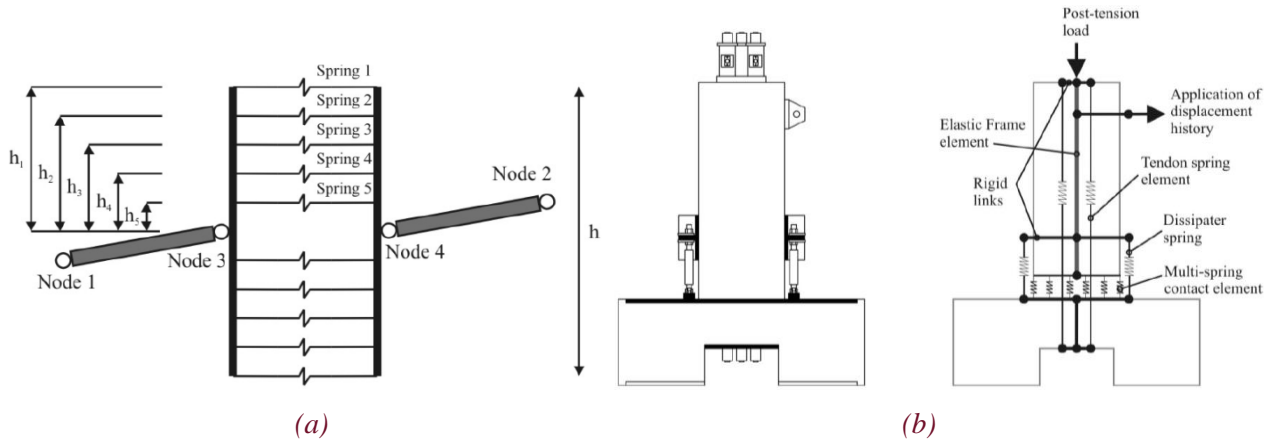


Figure 2: Multi-spring model (a) Ruaumoko (Carr 2004), (b) Cantilever rocking pier (Marriott 2009)

1.3 Fibre Element Model

Fibre models were developed to predict the response of rocking beam-column joints. Past research on this type of modelling include (Kurama et al. 1999). In fibre modelling, an element is divided into several segments which are consisted of discrete fibre layers. The fibres represent specific material (concrete or dissipaters) and its uniaxial stress-strain relationship. When the element starts rocking, the uplift (gap opening) is calculated by integrating the tension strain along the length of each segment. This type of modelling has been used by (Kurama 2000) and (Allen and Kurama 2002) to model the response of post-tensioned rocking walls with energy dampers. Fibre element models require specific software package and can be complicated to develop.

1.4 Finite Element Model

The finite element model requires modelling of the elements and joints in a finite element (FE) software package. The rocking interface is modelled using gap/contact element which would allow the uplift. Past research investigations have shown that the finite element model is well correlated to its equivalent fibre element model (Marriott 2009). Finite element models are generally sophisticated and require considerable amount of time to develop and run analysis.

2 ANALYTICAL MODELING OF A BRIDGE BENT WITH DCR CONNECTIONS

The procedure outlined in the PRESSS Design Handbook (Pampanin et al. 2010) for lumped plasticity modelling has been utilized to obtain the response of a bent with DCR connections. A fully precast half-scale bent with two columns was tested under uni-directional quasi-static cyclic loading. Figure 3 provides details of the bent and testing setup. The bent was tested under several DCR configurations (Fig. 4). This included testing of the bent with:

1. Three levels of initial post-tensioning (IPT) without any dissipaters or axial loads
 - a. IPT15-EX: IPT Force = 15% of the yield strength of the post-tensioning bar
 - b. IPT30-EX: IPT Force = 30% of the yield strength of the post-tensioning bar
 - c. IPT45-EX: IPT Force = 45% of the yield strength of the post-tensioning bar
2. IPT11.8+GD+AX: IPT = 11.8% plus grooved dissipaters (GD) and axial load (AX)

3. IPT9+MUD+AX: IPT = 9% plus mini UFP dissipaters (MUD) and axial load
4. IPT11.4+MUD+GD+AX: IPT = 11.4% plus mini UFP and grooved dissipaters and axial load

More information on the grooved and mini UFP dissipaters can be found in (Mashal et al. 2014), (White and Palermo 2016), and (Mashal and Palermo 2019).

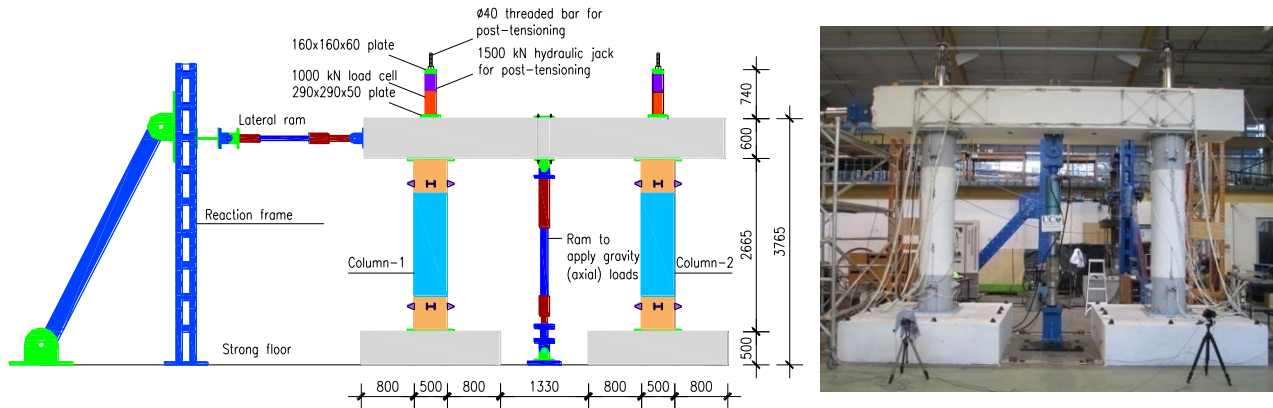


Figure 3: Details and testing setup for the precast bent with DCR connections

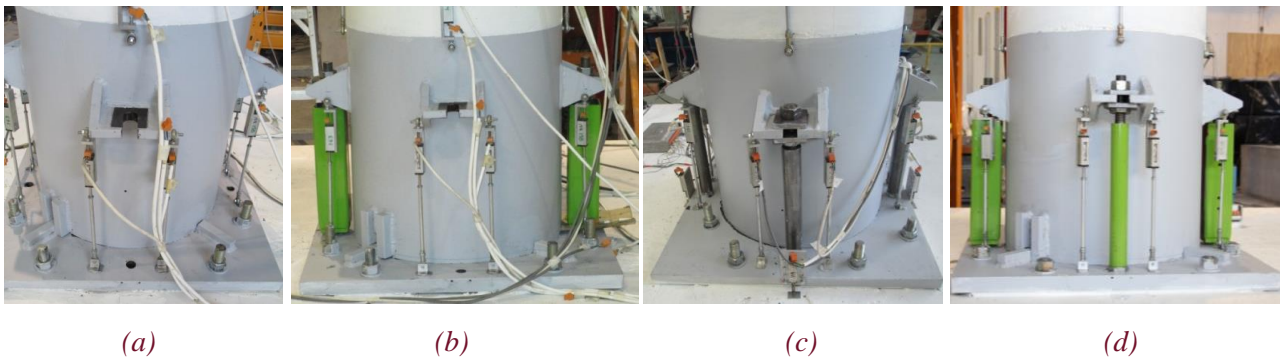


Figure 4: Typical DCR connection (a) without dissipaters, (b) mini UFP dissipaters, (c) grooved dissipaters, (d) mini UFP and grooved dissipaters

For simplified analytical modelling of the bent, the structure can be assumed as four short cantilever columns, each with a DCR connection at the base. The height of the cantilever column can be measured from the contraflexure point. The total capacity and displacement of the bent would be that of the short cantilever column times two, given the fact that all DCR connections incorporate identical detailing which was the case in this research. The monotonic behaviour (backbone curve) of a DCR connection can be obtained using the section analysis procedure titled "Monolithic Beam Analogy" (Pampanin et al. 2001) and (Palermo 2004). In this procedure, member compatibility condition is used to provide a compatibility equation for the DCR connection. In this analogy two beams have identical section and reinforcement details, and hence the elastic deformation in both beams is assumed to be the same. This means that when imposing an identical total displacement to each beam, the plastic deformation is also similar with difference in the mechanism only. For the precast beam with DCR connection, the nonlinear deformation is concentrated at the connection while for the monolithic beam the inelastic deformation is distributed along the plastic hinge length of the beam. The self-centring ratio (λ) is defined as follow:

$$\lambda = \frac{M_{pt} + M_N}{M_s} \quad (1)$$

Where in Equation 1, M_{pt} , M_s , and M_N are moment contribution from post-tensioned tendons, dissipaters, and gravity (axial load), respectively.

To generate the moment-rotation curve for each rotational spring in a typical DCR connection, three points (origin, yield level, and design level) are needed. Using the section analysis method, these points can be quickly calculated on a spreadsheet incorporating the formulas outlined in the PRESSS Design Handbook. The mathematical summation of the response from the rotational springs (dissipater, post-tensioning, axial load) will provide the backbone curve of the DCR connection. The cyclic response can be modelled using the data from the backbone, post-tensioning, and dissipater hysteresis plots.

2.1 Response with Post-Tensioning Only

As explained previously, three tests with initial post-tensioning (IPT) levels of 15%, 30%, and 45% of the yield force of the post-tensioning bar, were carried out. In this instance, there was no contribution from the external dissipaters and gravity. Using the PRESSS Design Handbook procedure, the backbone curve and cyclic response of the bent were modelled in a spreadsheet at the yield and ultimate limit state (ULS) levels. To simplify analysis, the decompression point (gap opening) was taken to be at zero displacement/force. Drift ratios at yield and ULS levels were taken/set from the design of the bent with DCR connections. Table 1 presents a summary of the calculated performance points for the bent under three levels of post-tensioning. It should be noted that since there are no dissipaters ($\lambda = \infty$), in reality there is no actual yield point. It is more a geometrical nonlinearity that is referred as “yield” in this instance due to rocking connections.

Table 1: Summary of the calculated performance points for the bent with post-tensioning only.

| Test Name | Design Drift (%) | | Force (kN) | |
|-----------------|------------------|-----|------------|-----|
| | Yield | ULS | Yield | ULS |
| IPT15-EX | | | 81 | 207 |
| IPT30-EX | 0.53 | 2.2 | 133 | 254 |
| IPT45-EX | | | 183 | 300 |

Figure 5a presents the moment-rotation plot for a typical DCR connection in the bent under IPT15-EX. The force-drift response is shown in Figure 5b. It can be noticed that the analytical model slightly over predicts the capacity of the bent at the ULS drift ratio. This was due to a very low level of post-tensioning which had caused some flexibility at the joints. The enclosed area in Figure 5b could be due to friction, contact damping, and some sliding in the DCR connections until the shear key is engaged.

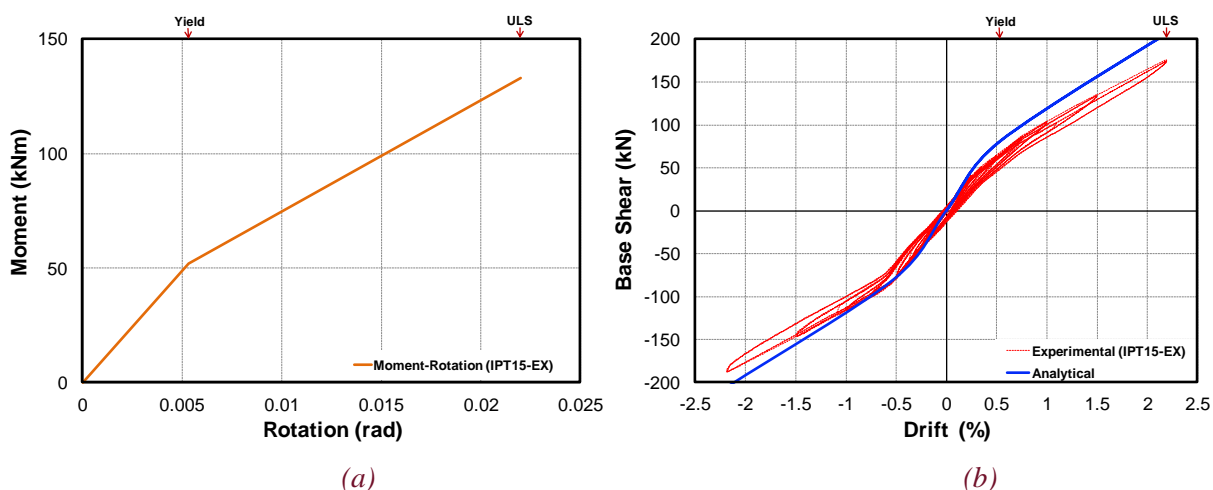


Figure 5: IPT15-EX (a) moment-rotation for one DCR connection, (b) hysteretic response of the bent

Analytical plots for the bent under IPT30-EX are presented in Figure 6. An increased level of post-tensioning in the bent had eliminated the flexibility in the bent. It can be observed that the analytical model in Figure 6b captures the response of the bent to a good level of accuracy, especially during the push stage of the loading.

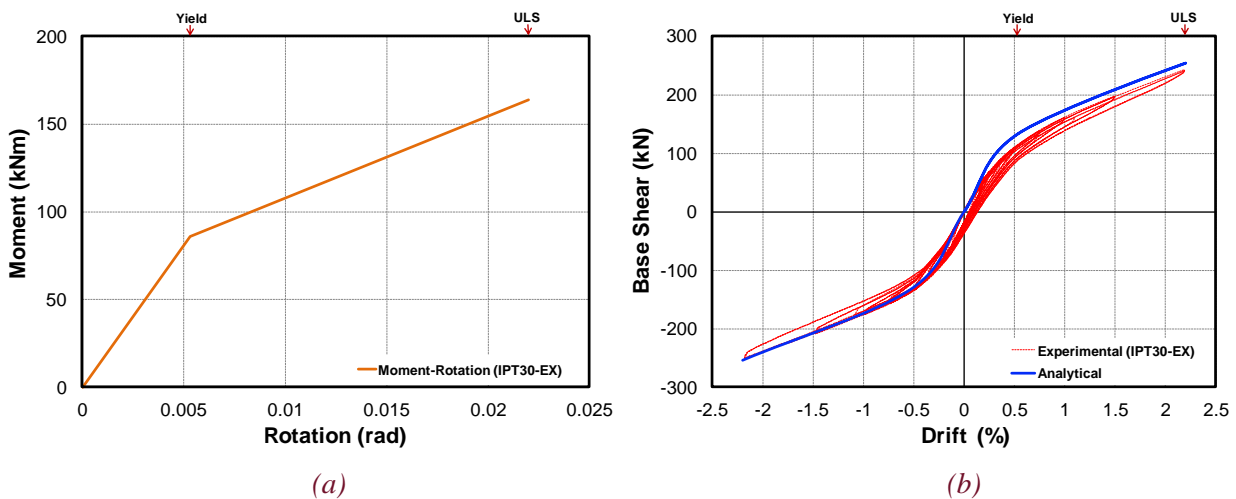


Figure 6: IPT30-EX (a) moment-rotation for one DCR connection, (b) hysteretic response of the bent

Results for testing of the bent under IPT45-EX are plotted in Figure 7. The moment-rotation plot for one of the DCR connections is presented in Figure 7a. The analytical model in Figure 7b well correlates with the experimental results. The slight asymmetry in experimental data was due to some out-of-plane movement in the bent as it was not braced in that direction. The simplified analytical procedure used in this paper does not take into account this movement.

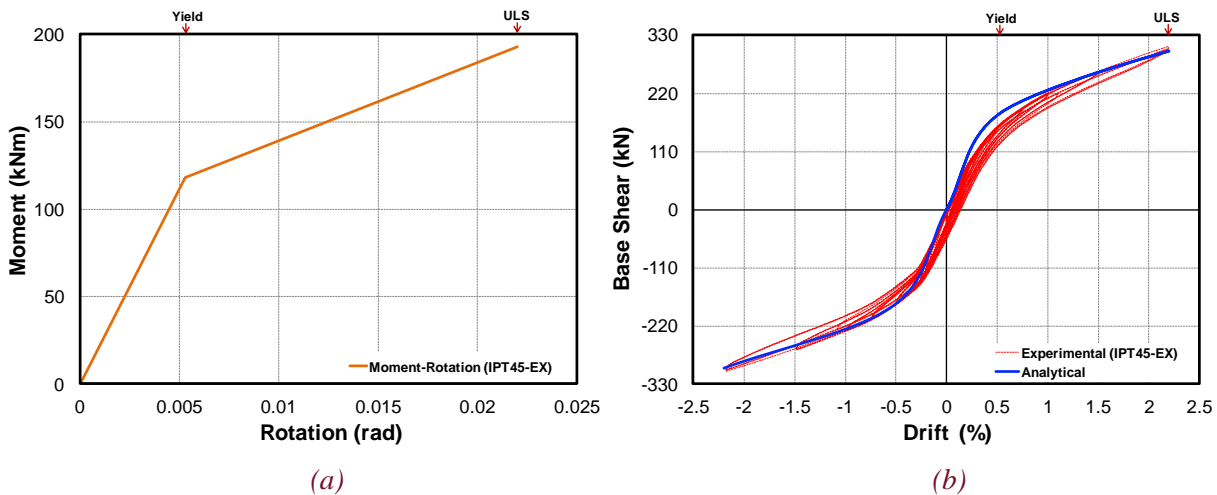


Figure 7: IPT45-EX (a) moment-rotation for one DCR connection, (b) hysteretic response of the bent

2.2 Response with Grooved Dissipaters

The response of the bent with grooved dissipaters (IPT11.8+GD+AX) was analytically modelled up to the 2.5% drift ratio (drift at the end of testing). The moment contributions from grooved dissipaters and gravity (axial load) were taken into account toward moment capacity of the DCR connection. The dissipaters were modelled using a simplified bilinear hysteretic rule (Fig. 8a). The hysteretic response of the unbonded post-tensioning was combined with gravity and is plotted in Figure 8b. Table 2 provides a summary of the calculated performance points for the combined flag-shaped response of the bent under IPT11.8+GD+AX.

Table 2. Summary of the calculated performance points for the bent with grooved dissipaters.

| Levels | Design Drift (%) | Force (kN) |
|--------|------------------|------------|
| Yield | 0.53 | 205 |
| ULS | 2.2 | 369 |
| MCE | 2.5 | 388 |

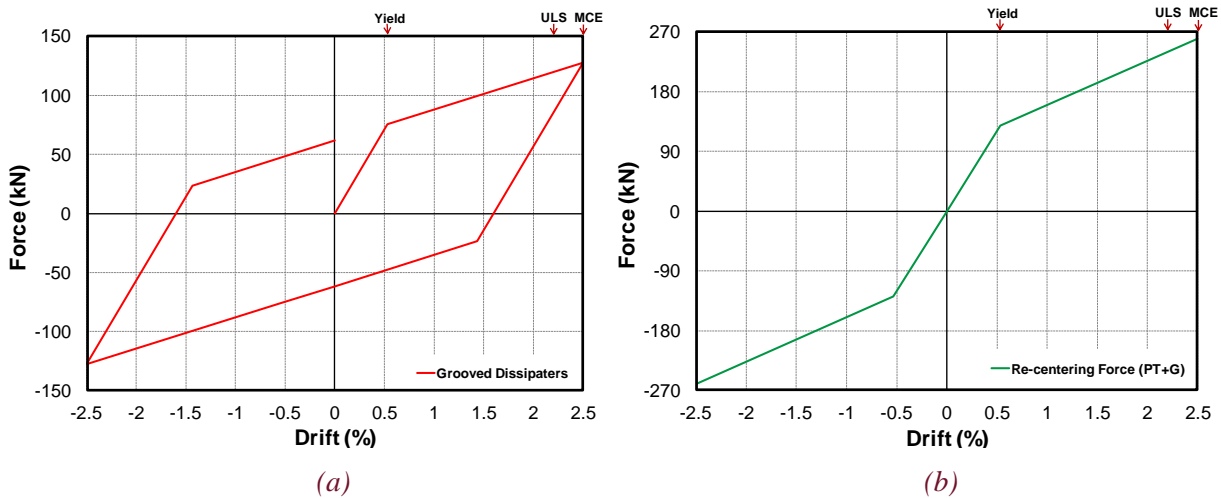


Figure 8: Typical DCR connection response under IPT11.8+GD+AX (a) grooved dissipaters, (b) post-tensioning and gravity combined (axial load)

The maximum considered earthquake (MCE) level drift in all tests was taken as the final drift that the bent was tested under. Figure 9a presents the moment-rotation plot for one of the four identical DCR connections in the bent. The analytical backbone curve of the overall bent is shown in Figure 9b which is in good agreements with experimental results.

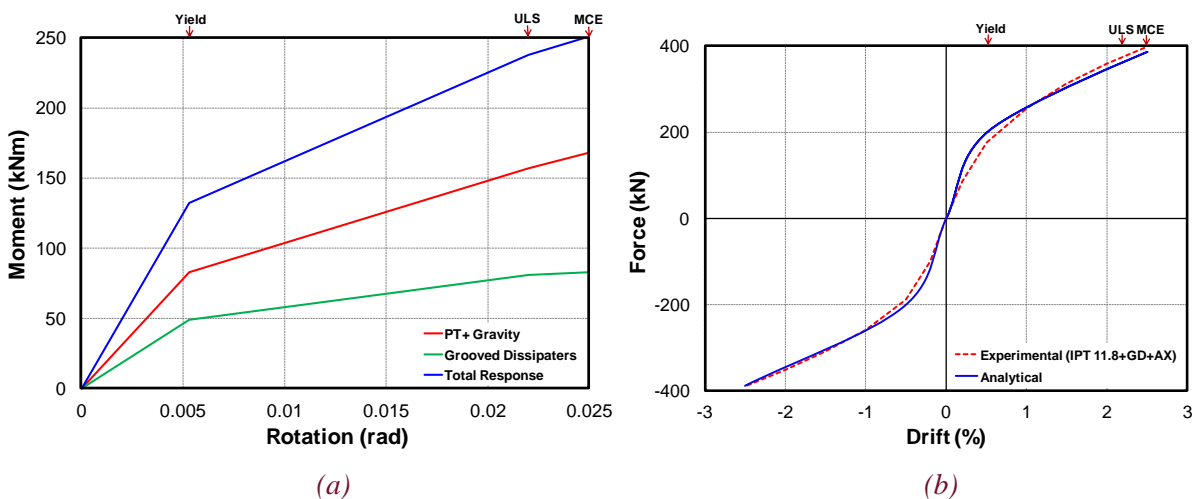


Figure 9: IPT11.8+GD+AX (a) moment-rotation for one DCR connection, (b) backbone curve of the bent

The analytical force-drift hysteresis of the bent is plotted in Figure 10. There was approximately 3 mm construction gap (0.1% drift ratio) between the face of the external shear key and outer face of the column in each DCR connection in the bent. The analytical model in Figure 10 does not take into account this gap. Therefore, it appears that following testing, the bent had slightly higher residual drift (0.25% drift ratio) compared to the analytical model. By subtracting 0.1% (gap width) from 0.25% drift, the actual residual drift in the bent was in the order of 0.15% or 4 mm. This residual drift is almost equal to that shown in the

analytical model in Figure 10. In general, the simplified analytical model shows good correlation with the experimental results up to the 2.5% drift ratio.

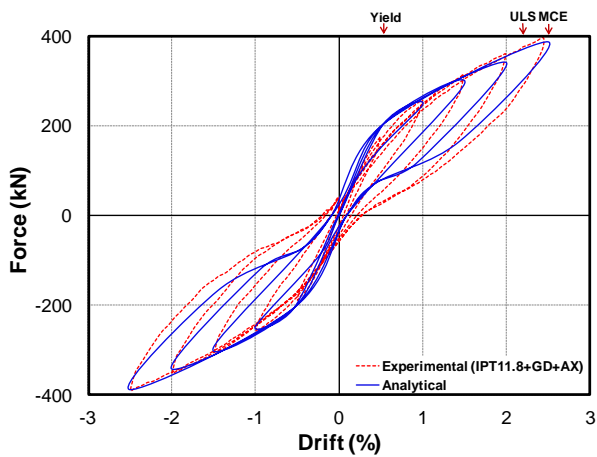


Figure 10: Force-drift hysteresis of the bent under IPT11.8+GD+AX.

2.3 Response with Mini UFP Dissipaters

The response of the bent under IPT9+MUD+AX can be modelled similar to that presented with grooved dissipaters in the previous section. The contribution of mini UFP dissipaters (MUDs) was computed using a bilinear model. A summary of the calculated performance points for the combined flag-shaped response of the bent under IPT9+MUD+AX is presented in Table 3. Analytical plots are presented in Figures 11-13.

Table 3. Summary of the calculated performance points for the bent under IPT9+MUD+AX.

| Levels | Design Drift (%) | Force (kN) |
|--------|------------------|------------|
| Yield | 0.53 | 122 |
| ULS | 2.2 | 264 |
| MCE | 2.5 | 288 |

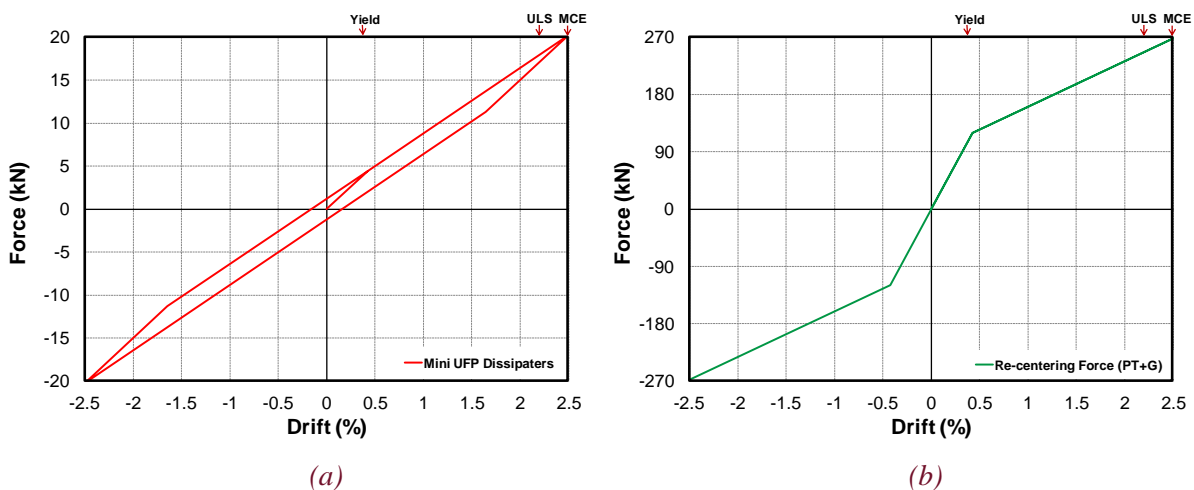


Figure 11: Typical DCR connection response under IPT9+MUD+AX (a) mini UFP dissipaters, (b) post-tensioning and gravity combined (axial load)

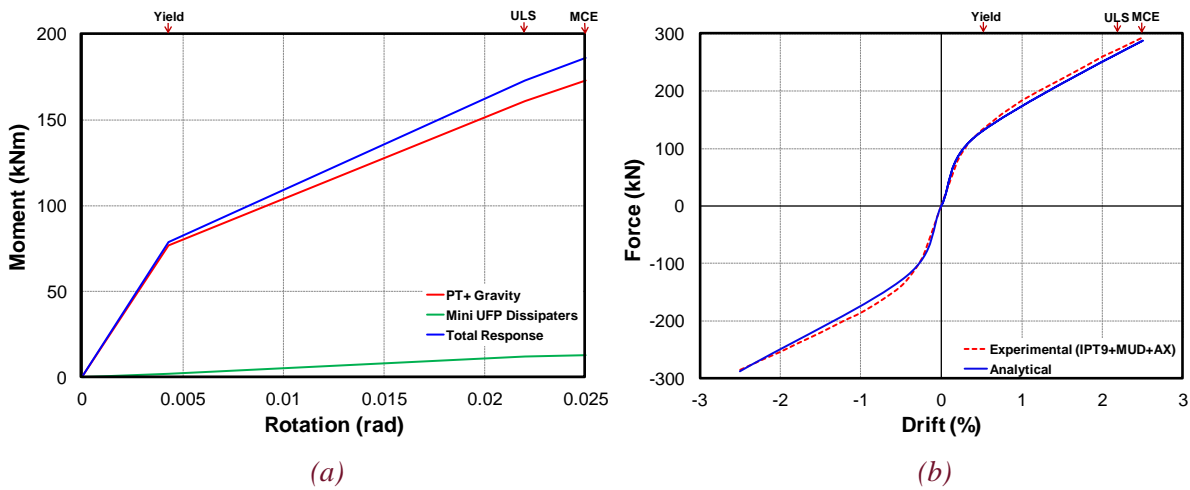


Figure 12: IPT9+MUD+AX (a) moment-rotation for one DCR connection, (b) backbone curve of the bent

In Figure 13a, the low capacity of the dissipaters was due to in-house fabrication constraints, only thinner UFPs could be rolled to build the dissipaters. Analytical results shown in Figures 12b and 13 are in good agreements with experimental results.

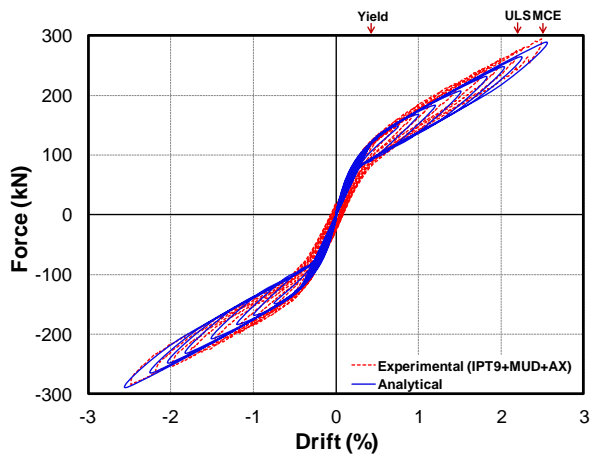


Figure 13: Force-drift hysteresis of the bent under IPT9+MUD+AX

2.4 Response with Grooved and Mini UFP Dissipaters

In this part, the response of the bent under IPT11.4+MUD+GD+AX is presented. The total response of a typical DCR connection includes moment contributions from grooved dissipaters (GDs), mini UFP dissipaters (MUDs), post-tensioning, and gravity (axial load). Table 4 presents a summary of the calculated performance points for the combined flag-shaped response of the bent under IPT 11.4+MUD+GD+AX. Moment contributions from MUDs and GDs are combined into a single plot (Fig. 14a). The hysteretic response of the combined unbonded post-tensioning and gravity is plotted in Figure 14b.

Table 4. Summary of the calculated performance points for the bent under IPT11.4+MUD+GD+AX.

| Levels | Design Drift (%) | Force (kN) |
|--------|------------------|------------|
| Yield | 0.53 | 149 |
| ULS | 2.2 | 315 |
| MCE | 3.0 | 362 |

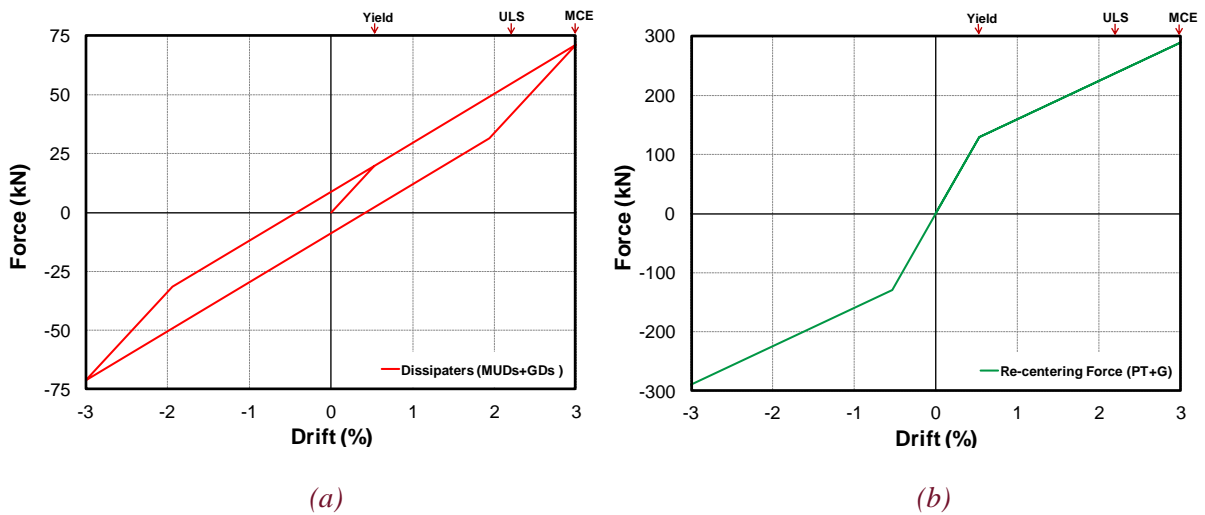


Figure 14: Typical DCR connection response under IPT11.4+MUD+GD+AX (a) mini UFP and grooved dissipaters, (b) post-tensioning and gravity combined (axial load)

The moment-rotation and backbone plots are shown in Figure 15a and Figure 15b, respectively. The force-drift hysteresis is plotted in Figure 16.

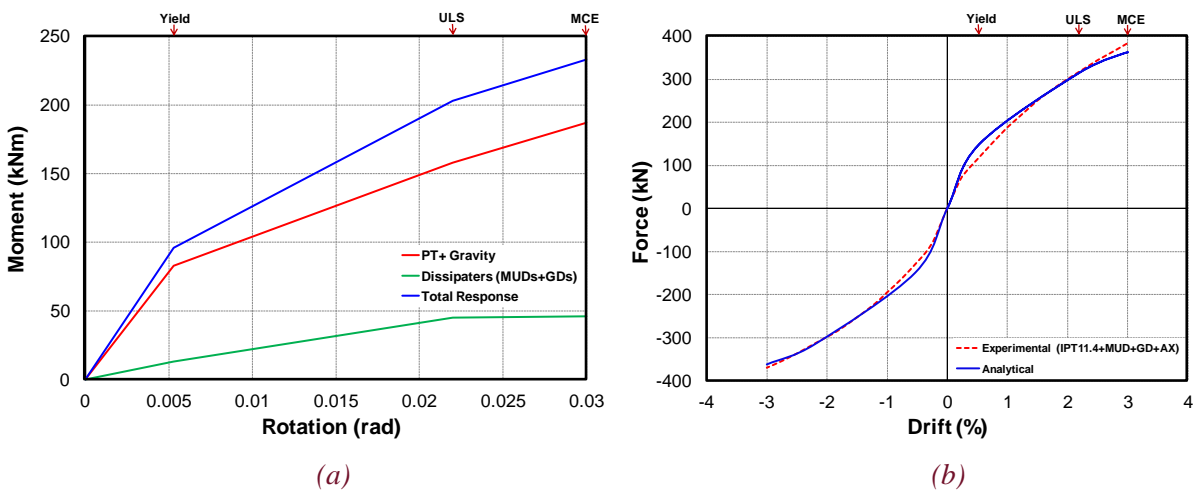


Figure 15: IPT11.4+MUD+GD+AX (a) moment-rotation for a DCR joint, (b) backbone curve of the bent

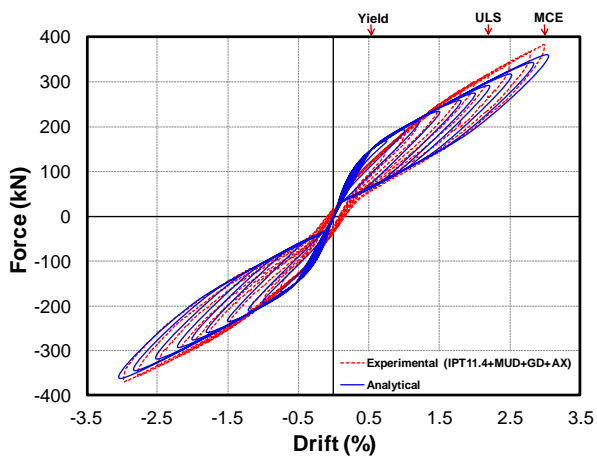


Figure 16: Force-drift hysteresis of the bent under IPT11.4+MUD+GD+AX

3 CONCLUSIONS

The response of a precast bent with dissipative controlled rocking (DCR) connections was modelled using simplified lumped plasticity models presented in the PRESSSS Design Handbook. The bent in this research had two columns. Each column in the bent was thought as two short cantilever columns with DCR connections at the base. The height of the cantilever column can be measured from the contraflexure point. All DCR connections in the bent had similar detailing. Therefore, the total capacity of the bent was approximated by multiplying the computed capacity of a short cantilever column by two. The total displacement in the bent was the summation of the displacement from each short cantilever column. A typical DCR connection was modelled using two rotational springs placed parallel to each other at the rocking interface. One spring represented the unbonded post-tensioning while the other represented the dissipaters. The dissipaters were modelled using simple bilinear response approach. The effects of gravity (axial load) was considered and added to the spring representing the unbonded post-tensioning. The overall response of the DCR connection was obtained by summing the contributions from the two rotational springs. Using the procedure above, the analytical backbone curve and cyclic response of the bent were plotted for a variety of post-tensioning, axial load, and dissipaters' arrangement. Analytical results showed good correlation with the experimental data. Lumped plasticity models provide simple and efficient analytical modelling of bridges with DCR connections. They can be incorporated in a spreadsheet. However, these models provide macro-level information, and therefore have limited capabilities.

4 REFERENCES

- Allen, M.G. & Kurama, Y.C. 2002. Design of Rectangular Openings in Precast Walls Under Combined Vertical and Lateral Loads, *PCI Journal*.
- Carr, A. 2004. *RUAUMOKO program for inelastic dynamic analysis*.
- Conley, J., Sritharan, S. & Priestley, M.J.N. 1999. *Precast Seismic Structural Systems PRESSSS-3: The Five-Story Precast Test Building*, Vol 3-5, Wall direction response. Report SSRP-99/19.
- Group, T. 2003. *Seismic design of precast concrete building structures*, Civil Engineering.
- Kim, J. 2002. *Behavior of hybrid frames under seismic loading*, ProQuest Dissertations and Theses, University of Washington.
- Kurama, Y.C. 2000. Seismic design of unbonded post-tensioned precast concrete walls with supplemental viscous damping, *ACI Structural Journal*.
- Kurama, Y., Pessiki, S., Sause, R. & Lu, L.-W. 1999. Seismic Behavior and Design of Unbonded Post-Tensioned Precast Concrete Walls, *PCI Journal*.
- Marriott. 2009. *The Development of High-Performance Post-Tensioned Rocking Systems for the Seismic Design of Structures*, Doctoral Dissertation, University of Canterbury.
- Mashal M., Palermo A. & K. G. 2019. Innovative dissipaters for earthquake protection of structural and non-structural components, *Soils Dynamics and Earthquake Engineering*, Vol 116 31–42.
- Mashal, M., White, S. & Palermo, A. 2014. Accelerated bridge construction and seismic low-damage technologies for short-medium span bridges, *37th IABSE Symposium on Engineering for Progress, Nature and People*, 1208–1215.
- Palermo, A., Pampanin, S. & Calvi, G.M. 2004. Use of 'Controlled Rocking' in the seismic design of Bridges, *13th World Conference on Earthquake Engineering*.
- Palermo, A., Pampanin, S. & Calvi, G.M. 2005a. Concept and development of hybrid solutions for seismic resistant bridge systems, *Journal of Earthquake Engineering*, Vol 9(6) 899–921.
- Palermo, A., Pampanin, S. & Carr, A. 2005b. Efficiency of simplified alternative modelling approaches to predict the seismic response of precast concrete hybrid systems, *fib Symposium "Keep Concrete Attractive."*
- Pampanin, S., Marriot, D. & Palermo, A. 2010. *PRESSSS Design Handbook*, New Zealand Concrete Society (NZCS) Incorporation.
- Pampanin, S., Nigelpriestley, M.J. & Sritharan, S. 2001. Analytical modelling of the seismic behaviour of precast

concrete frames designed with ductile connections, *Journal of Earthquake Engineering*.

Spieth, H.A., Carr, A.J., Murahidy, A.G., Arnolds, D., Davies, M. & Mander, J.B. 2004. Modelling of post-tensioned precast reinforced concrete frame structures with rocking beam-column connections, *New Zealand Society of Earthquake Engineering Conference 2004*.

White, S. & Palermo, A. 2016. Quasi-Static Testing of Posttensioned Nonemulative Column-Footing Connections for Bridge Piers, *Journal of Bridge Engineering*.